JOURNAL OF GUIDANCE, CONTROL, AND DYNAMICS
Vol. 33, No. 4, July–August 2010

Coning Algorithm Design by Explicit Frequency Shaping

Paul G. Savage*
Strapdown Associates, Inc., Maple Plain, Minnesota 55359

DOI: 10.2514/1.47337

A new optimum approach is presented for strapdown coning algorithm design based on Explicit matching of desired response to expected coning input magnitude as a function of coning frequency. Unlike previous time or frequency Taylor series expansion techniques, the new method achieves optimization through minimum least-squares estimation over a user selected design frequency range. The error being minimized is the square of the weighted algorithm error, the weighting factor being user specified coning amplitude over frequency. This methodology allows the coning algorithm coefficients to be independently designed for each coning axis to achieve optimal balanced performance over the frequency range of expected coning inputs. Performance of the new algorithm design technique is evaluated by comparison with previous time and frequency-series approaches, in discrete and stochastic coning environments, and over a time based extreme dynamic maneuvering profile. A generalized method is presented for translating system performance requirements into expected coning amplitude versus frequency profiles for calculating Explicit algorithm coefficients, and for evaluating coning algorithm accuracy. The paper includes derivations of generalized formulas for calculating algorithm coefficients for previous time and frequency-series design approaches.

Introduction

MODERN day strapdown inertial navigation attitude updating algorithms have been based on a general two-stage structure introduced by Jordan [1] and Bortz [2] in 1969: an exact routine is used to update each attitude update cycle; the input to the updating routine is a rotation vector equal to integrated gyro sensed angular rotation rate over the attitude update cycle plus a coning correction calculated from gyro data in a separate algorithm executed between update cycles. In Jordan [1] the coning correction algorithm was based on an approximation to the Goodman/Robinson theorem [3]. In Bortz [2,4] the coning correction was based on the integrated Laning rotation vector rate equation [5]. Both approaches are analytically equivalent. Since 1971, attitude algorithm design activity has centered on developing routines for computing the coning correction using various approximations to the integrated rotation vector rate equation.

Early algorithms for the coning correction were based on truncated Taylor time-series expansion approximations for sensed angular rate over the coning algorithm computation interval (see Appendix A for a general treatment of this approach). In 1983, Miller [6] introduced the concept of designing the coning correction algorithm for optimum performance in a pure coning environment. This was achieved using a truncated Taylor series expansion formulation in powers of coning frequency (rather than time). In 1990 and 1996, Ignagni [7,8] expanded the Miller frequency-series concept using a simplified development approach and an interesting property of coning motion (that cross products between time displaced integrated rate samples are a function of only displacement time). References [7,8] also analytically demonstrated that algorithm design for optimum pure coning performance is achievable for negligible performance penalty in dynamic maneuver environments (for which time-series solutions still excel).

This paper introduces a new concept for coning algorithm design that achieves balanced optimal performance over the frequency range of expected coning inputs. The new approach (denoted herein as Explicit frequency shaping) uses least-squares error minimization (rather than frequency or time Taylor series expansion) to achieve optimal performance over a design frequency range. The general structure of Explicit frequency shaping allows tailoring for expected coning environments. The design coning environment can be specified discrete amplitude as a function of frequency or stochastically as a power spectrum. Alternatively, the technique can be applied in the traditional manner for optimal design over a uniform constant coning versus frequency profile.

Performance characteristics are evaluated for the Explicit approach and compared with the equivalent times-series and frequency-series methods under discrete coning rate inputs, coning motion generated in a stochastic dynamic environment, and under an extreme dynamic time based maneuver profile. Algorithm performance for discrete coning inputs is presented as computed attitude bias drift error versus frequency. For comparison, the equivalent normalized error response is provided (i.e., algorithm error versus frequency for unity coning amplitude). A section is included illustrating how expected coning values can be generated for a given application based on specified system level performance requirements and the dynamic response characteristics of the strapdown sensor assembly mechanical isolator mounting configuration.

Attitude Computation Forms

The classical attitude updating computational form used in modern day strapdown inertial navigation systems (e.g., [1,2,4,12,13] and [9], section 7.1.1) is given by

$$C_l = C_{l-1}[I + f_1(\phi_l)(\underline{\phi}_l\times) + f_2(\phi_l)(\underline{\phi}_l\times)^2]$$

$$f_1(\phi_l) = \frac{\sin\phi_l}{\phi_l} = \sum_{i=1}(-1)^{i-1}\frac{\phi_l^{2(i-1)}}{(2i-1)!}$$

$$f_2(\phi_l) = \frac{1}{\phi_l^2}(1-\cos\phi_l) = \sum_{i=1}(-1)^{i-1}\frac{\phi_l^{2(i-1)}}{(2i)!} \tag{1}$$

where C is an attitude orientation direction cosine matrix that transforms vectors from a coordinate frame aligned with the system angular-rate sensors (gyros) into a navigation coordinate frame, $\underline{\phi}_l$ is a rotation vector for computation cycle l used to update C from its value at the end of cycle $l-1$ to its value at the end of cycle l, and the cross-product operator $(\underline{\phi}_l\times)$ is

$$\begin{bmatrix} 0 & -\phi_z & \phi_y \\ \phi_z & 0 & -\phi_x \\ -\phi_y & \phi_x & 0 \end{bmatrix}$$

Received 24 September 2009; revision received 20 March 2010; accepted for publication 21 March 2010.

*Senior Member AIAA.

composed of $\underline{\phi}_l$ components. (An equivalent formulation is also commonly used whereby $\underline{\phi}_l$ is used to update attitude in the form of a quaternion.) The rotation vector $\underline{\phi}_l$ is calculated by computational routines designed to approximate the integral of the rotation vector rate equation. A commonly used approximation ([1,7,8,12,13] and [9] section 7.1.1.1) is the simplified form

$$\underline{\phi}_l = \underline{\alpha}_l + \delta\underline{\phi}_l \qquad \delta\underline{\phi}_l \approx \int_{t_{l-1}}^{t_l} \frac{1}{2}\underline{\alpha}(t - t_{l-1}) \times \mathrm{d}\underline{\alpha}$$
$$\underline{\alpha}(t - t_{l-1}) = \int_{t_{l-1}}^{t} \underline{\omega}\,\mathrm{d}t = \int_{t_{l-1}}^{t} \mathrm{d}\underline{\alpha} \qquad \underline{\alpha}_l = \underline{\alpha}(t = t_l) \tag{2}$$

where $\underline{\alpha}_l$ is the integrated gyro sensed angular rate $\underline{\omega}$ from time t_{l-1} to time t_l and $\delta\underline{\phi}_l$ has been denoted as the coning correction.

Because attitude updating Eq. (1) are exact, their accuracy is unaffected by the computation rate, which can be selected based on considerations other than accuracy (e.g., desired attitude output rate). Digital algorithmic forms of Eq. (2), however, have generally required a high computation rate to assure that high-frequency (but small amplitude) coning motion is accurately measured and calculated. The original motivation underlying the structure of Eq. (1) with Eq. (2) was to allow the more complex attitude update equations to be processed at a lower n cycle rate than the simpler rotation vector equations, thereby reducing net computer throughput while maintaining overall attitude computational accuracy. Such a two-speed structure was originated in 1966 ([10]) using a second order algorithm for attitude updating. Many strapdown algorithms have since employed the two-speed approach ([1,2,4,7,8,12,13] and [9] section 7.1.1) as represented by the following equivalent form of Eqs. (1) and (2):

$$C_n = C_{n-1}[I + f_1(\phi_n)(\underline{\phi}_n\times) + f_2(\phi_n)(\underline{\phi}_n\times)^2]$$
$$f_1(\phi_n) = \frac{\sin\phi_n}{\phi_n} = \sum_{i=1}(-1)^{i-1}\frac{\phi_n^{2(i-1)}}{(2i-1)!}$$
$$f_2(\phi_n) = \frac{1}{\phi_n^2}(1-\cos\phi_n) = \sum_{i=1}(-1)^{i-1}\frac{\phi_n^{2(i-1)}}{(2i)!}$$
$$\underline{\phi}_n = \underline{\alpha}_n + \delta\underline{\phi}_n$$
$$\delta\underline{\phi}_n = \int_{t_{n-1}}^{t_n}\frac{1}{2}\underline{\alpha}(t-t_{n-1})\times\mathrm{d}\underline{\alpha} = \sum_{t_{n-1}}^{t_n}\left(\frac{1}{2}\underline{\alpha}_{m-1}\times\Delta\underline{\alpha}_l + \delta\underline{\phi}_l\right)$$
$$\underline{\alpha}_m = \sum_{t_{n-1}}^{t_m}\Delta\underline{\alpha}_l \qquad \underline{\alpha}_0 = 0 \qquad \underline{\alpha}_n = \underline{\alpha}_m(t_m = t_n)$$
$$\delta\underline{\phi}_l \approx \int_{t_{l-1}}^{t_l}\frac{1}{2}\underline{\alpha}(t-t_{l-1})\times\mathrm{d}\underline{\alpha} \qquad \underline{\alpha}(t-t_{l-1}) = \int_{t_{l-1}}^{t}\mathrm{d}\underline{\alpha}$$
$$\underline{\alpha}_l = \underline{\alpha}(t = t_l) \tag{3}$$

Note that Jordan [1] applied the two-speed approach as a digital computer algorithm; Bortz [2,4] incorporated the two-speed approach as an analog biasing feedback signal to the system gyros.

Equation (3) are entirely equivalent to Eqs. (1) and (2) producing identical results (except for the previously discussed minor approximation errors in the simplified form of the coning integral over an attitude update cycle that forms the basis for the algorithm design). The remainder of this paper deals with the Eqs. (1) and (2) forms with the understanding that the Eq. (3) two-speed structure can be used as an alternate if needed to reduce computer throughput. Because of the high-speed, long word length, floating point arithmetic capabilities of modern day computers (for high throughput with negligible roundoff error), the Eq. (3) form may no longer be needed in many applications. Note that the $\delta\underline{\phi}_l$ expression is identical in Eqs. (2) and (3). As such, the computation algorithms to be discussed for $\delta\underline{\phi}_l$ can be applied unchanged to the Eqs. (1) and (2) or the two-speed Eq. (3) form. The Roscoe conversion formula [Eq. (11)] shows how they can also be applied to sculling algorithms incorporated in strapdown inertial navigation system (INS) acceleration transformation operations.

Coning Algorithm Structure

Computational algorithms used for the coning correction $\delta\underline{\phi}_l$ element in Eq. (2) have generally had the form ([7,8,12,13] and [9] section 10.1.1.2.2):

$$\delta\underline{\phi}_{\mathrm{Algo}_l} = \sum_{j=1}^{N-1}\sum_{i=j+1}^{N}\varsigma_{ij}\Delta\underline{\alpha}_i\times\Delta\underline{\alpha}_j \tag{4}$$

where each $\Delta\underline{\alpha}$ is an integrated gyro angular-rate sample over a specified sample time, the $\varsigma_{ij}s$ are constants whose values depend on the algorithm design approach, and N is the number of $\Delta\underline{\alpha}$ samples used in the $\delta\underline{\phi}_{\mathrm{Algo}_l}$ calculation. Note that each term in Eq. (4) has the same property as the $\delta\underline{\phi}_l$ integrand in Eq. (2); each is identically zero when the angular-rate axis maintains a fixed orientation in inertial space (for which the $\Delta\underline{\alpha}s$ remain parallel). Thus, the general $\delta\underline{\phi}_{\mathrm{Algo}_l}$ structure in Eq. (4) [as in Eq. (2)] only responds to angular motion where the angular-rate axis is rotating in inertial space (the analytical definition of coning).

Strapdown systems are generally configured to form the $\Delta\underline{\alpha}$ integrals over a fixed sample time interval t_{k-1} to t_k at a k cycle sample rate equal to or faster than the l cycle $\delta\underline{\phi}_l$ computation rate. The $\Delta\underline{\alpha}s$ for Eq. (4) are adjacent and spaced sequentially backward in time from time t_l. With this structuring, $\delta\underline{\phi}_{\mathrm{Algo}_l}$ in Eq. (4) and the integrated angular-rate $\underline{\alpha}_l$ portion of the Eq. (2) $\underline{\phi}_l$ calculation is given by

$$\delta\underline{\phi}_{\mathrm{Algo}_l} = \sum_{j=1}^{N-1}\sum_{i=j+1}^{N}\varsigma_{ij}\Delta\underline{\alpha}_{k+1-i}\times\Delta\underline{\alpha}_{k+1-j} \tag{5}$$

$$\underline{\alpha}_l = \sum_{s=1}^{L_{kl}}\Delta\underline{\alpha}_{k+1-s} \tag{6}$$

The N value in Eq. (5) is selected to be equal or greater than L_{kl}, the number of k cycles in an l cycle, thereby assuring that the $\Delta\underline{\alpha}s$ will as a minimum include all samples generated over the l cycle (from t_{l-1} to t_l). For L_{kl} greater than one and Eq. (5) applied within a two-speed Eq. (3) structure, the overall configuration has been designated as a three-speed computation approach. The first use of the three-speed approach was by Jordan [1] using $L_{kl} = N = 2$.

Miller [6] first introduced the concept of basing ς_{ij} coefficient design on matching Eq. (5) to the coning response in a classical coning angular-rate $\underline{\omega}$ environment at coning frequency Ω

$$\underline{\omega} = \underline{u}_a\theta_{0_a}\Omega\cos\Omega t + \underline{u}_b\theta_{0_b}\Omega\sin\Omega t \tag{7}$$

where $\underline{u}_a$, $\underline{u}_b$ are mutually orthogonal unit vectors and θ_{0_a}, θ_{0_b} are angular amplitudes of the oscillatory motion generated by $\underline{\omega}$ around $\underline{u}_a$ and $\underline{u}_b$ [i.e., the integral of Eq. (7)]. It has been well known ([7,8] and [9] section 10.1.1.2.2) that for $\Delta\underline{\alpha}$ samples of the same time width in an Eq. (7) type coning environment, all $\Delta\underline{\alpha}_i\times\Delta\underline{\alpha}_j$ products with the same time spacing between i and j samples are equal. Based on this property, Ignagni [8] defined a simplified version of Eq. (5) for the coning correction algorithm:

$$\delta\underline{\phi}_{\mathrm{Algo}_l} = \sum_{s=1}^{N-1}C_s(\Delta\underline{\alpha}_{k-s}\times\Delta\underline{\alpha}_k) = \left(\sum_{s=1}^{N-1}C_s\Delta\underline{\alpha}_{k-s}\right)\times\Delta\underline{\alpha}_k \tag{8}$$

The C_s coefficients in Eq. (8) are the combined equivalent of the $\varsigma_{ij}s$ in Eq. (5) under Eq. (7) coning rate inputs, viz.:

$$C_s = \sum_{i=s+1}^{N}\varsigma_{i,i-s} \tag{9}$$

Recent frequency based coning algorithms (e.g., [8] and the Explicit approach) use Eq. (8) for the coning correction when

computing the Eq. (2) rotation vector; the $\underline{\alpha}$ integrated rate component is calculated from cumulative $\Delta\underline{\alpha}$ samples as in Eq. (6).

Coefficient Design by Explicit Frequency Shaping

The theoretical basis for the Explicit as with other frequency-based coning algorithm design approaches originates from the characteristics of angular motion under coning type angular rates. In an Eq. (7) pure coning environment, direct analytical integration of Eqs. (2) shows that the $\delta\underline{\phi}_l$ coning correction term is directed along an axis $\underline{u}_c$ perpendicular to the orthogonal $\underline{u}_a$, $\underline{u}_b$ unit vectors with magnitude $\delta\phi_l$ given by

$$\delta\phi_l = \dot{\Phi}(\Omega)\left(1 - \frac{\sin(\Omega T_l)}{\Omega T_l}\right)T_l \qquad \dot{\Phi}(\Omega) \equiv \frac{1}{2}\Omega\theta_{0_a}\theta_{0_b} \tag{10}$$

where $\dot{\Phi}(\Omega)$ is the steady total rotation (coning) rate around $\underline{u}_c$ of the sensor assembly attitude orientation (the C matrix in Eq. (1)) in response to the Eq. (7) angular rate, and T_l is the time interval from t_{l-1} to t_l. In an Eq. (7) coning environment it is also widely recognized ([7,8] and [9] section 10.1.1.2.2) that the magnitude of the $\Delta\underline{\alpha}_{k-s} \times \Delta\underline{\alpha}_k$ terms in Eq. (8) is $2\dot{\Phi}(\Omega)f_s(\beta)\ T_k$, in which

$$f_s(\beta) = 2s\frac{\sin s\beta}{s\beta} - (s-1)\frac{\sin(s-1)\beta}{(s-1)\beta} - (s+1)\frac{\sin(s+1)\beta}{(s+1)\beta}$$
$$\beta \equiv \Omega T_k \tag{11}$$

where T_k is the sensor sample time interval from t_{k-1} to t_k, and β is a T_k normalized frequency parameter. Thus, the magnitude of $\delta\underline{\phi}_{\mathrm{Algo}_l}$ in Eq. (8) is

$$\delta\phi_{\mathrm{Algo}_l}(\Omega) = 2\dot{\Phi}(\Omega)T_k\sum_{s=1}^{N-1} C_s f_s(\beta) \tag{12}$$

The desired output from the coning correction algorithm $\delta\phi_{\mathrm{Desired}_l}(\Omega)$ is the Eq. (10) $\delta\phi_l$ response

$$\delta\phi_{\mathrm{Desired}_l}(\Omega)\dot{\Phi}(\Omega) = \left(1 - \frac{\sin(\Omega T_l)}{\Omega T_l}\right)T_l$$
$$= \dot{\Phi}(\Omega)\left(1 - \frac{\sin(L_{kl}\beta)}{L_{kl}\beta}\right)L_{kl}T_k \tag{13}$$

where L_{kl} (the number of k cycles in an l cycle) is the ratio of k cycle sensor sampling to l cycle coning correction computation intervals ($L_{kl} = T_l/T_k$). We define the coning correction algorithm error $e_{\mathrm{Cone}_l}(\Omega)$ as the difference between the Eq. (12) $\delta\phi_{\mathrm{Algo}_l}$ algorithm response and $\delta\phi_{\mathrm{Desired}_l}(\Omega)$ in Eq. (13)

$$e_{\mathrm{Cone}_l}(\Omega) = \dot{\Phi}(\Omega)\left[2\left(\sum_{s=1}^{N-1} C_s f_s(\beta)\right) - \left(1 - \frac{\sin(L_{kl}\beta)}{L_{kl}\beta}\right)L_{kl}\right]T_k \tag{14}$$

Minimizing $e_{\mathrm{Cone}_l}(\Omega)$ in Eq. (14) has, in effect, been the design basis for previous frequency-series algorithms ([6–8]). The method was to expand Eq. (14) as a Taylor series in powers of normalized coning frequency and then design the algorithm C_s coefficients to null the Taylor series expansion coefficients. As a result, $e_{\mathrm{Cone}_l}(\Omega)$ in Eq. (14) becomes zero for the number of terms carried in the series. The series is truncated so that the number of terms carried matches the number of terms (and coefficients) used in the coning algorithm. The result is a set of null equations for the Taylor series coefficients that are solved simultaneously to determine the algorithm C_s coefficients. (See Appendix B for a general treatment of this approach.)

With the Explicit frequency shaping method, the C_s coefficients are also designed to minimize Eq. (14), but in a least-squares integral sense over a user selected frequency range. The coning amplitude term $\dot{\Phi}(\Omega)$ in (14) is retained as a means for weighting $e_{\mathrm{Cone}_l}(\Omega)$ in the minimization process (note that for the frequency-series design process, coning amplitude is eliminated from C_s determination when $e_{\mathrm{Cone}_l}(\Omega)$ in Eq. (14) is equated to zero for the Taylor series expansion). The error to be minimized with the Explicit approach is z, the integral of $e_{\mathrm{Cone}_l}(\Omega)$ squared over the user specified β frequency range β_{Range}

$$z \equiv \int_0^{\beta=\beta_{\mathrm{Range}}} [e_{\mathrm{Cone}_l}(\Omega)]^2\,\mathrm{d}\beta = \int_{\beta=0}^{\beta=\beta_{\mathrm{Range}}} \dot{\Phi}(\Omega)^2\left[2\left(\sum_{s=1}^{N-1} C_s f_s(\beta)\right) - \left(1 - \frac{\sin(L_{kl}\beta)}{L_{kl}\beta}\right)L_{kl}\right]^2 T_k^2\,\mathrm{d}\beta \tag{15}$$

Minimizing Eq. (15) takes the partial derivative with respect to each C_s and equates each to zero

$$\int_{\beta=0}^{\beta=\beta_{\mathrm{Range}}} \dot{\Phi}(\Omega)^2 f_r(\beta)\left[2\left(\sum_{s=1}^{N-1} C_s f_s(\beta)\right) - \left(1 - \frac{\sin(L_{kl}\beta)}{L_{kl}\beta}\right)L_{kl}\right]\mathrm{d}\beta = 0 \quad \text{or}$$
$$\sum_{s=1}^{N-1} C_s\left(\int_{\beta=0}^{\beta=\beta_{\mathrm{Range}}} 2\dot{\Phi}(\Omega)^2 f_r(\beta)f_s(\beta)\,\mathrm{d}\beta\right) = \int_{\beta=0}^{\beta=\beta_{\mathrm{Range}}} \dot{\Phi}(\Omega)^2 f_r(\beta)\left(1 - \frac{\sin(L_{kl}\beta)}{L_{kl}\beta}\right)L_{kl}\,\mathrm{d}\beta \tag{16}$$

Defining terms

$$a_{rs} \equiv \int_{\beta=0}^{\beta=\beta_{\mathrm{Range}}} 2\dot{\Phi}(\Omega)^2 f_r(\beta)f_s(\beta)\,\mathrm{d}\beta$$
$$b_r = \int_{\beta=0}^{\beta=\beta_{\mathrm{Range}}} \dot{\Phi}(\Omega)^2 f_r(\beta)\left(1 - \frac{\sin(L_{kl}\beta_k)}{L_{kl}\beta_k}\right)L_{kl}\,\mathrm{d}\beta \tag{17}$$

then gives

$$A\underline{C}_s = \underline{b} \tag{18}$$

where A is an $N-1$ by $N-1$ square matrix formed from a_{rs} elements, $\underline{C}_s$ is a column matrix whose elements are the C_s coefficients, and $\underline{b}$ is a column matrix formed from the b_r elements. Rearrangement of Eq. (18) provides the C_s coefficients

$$\underline{C}_s = A^{-1}\underline{b} \tag{19}$$

Equation (19) for $\underline{C}_s$ is then used in (8) to compute $\delta\underline{\phi}_{\mathrm{Algo}_l}$.

The previous development was based on Explicit coefficient optimization under specified discrete coning versus frequency conditions. The technique can be extended to also cover stochastic angular-rate environments in which coning might also be present (e.g., coning generated by a linear random vibration source that induces correlated angular motion about two orthogonal angular-rate sensor axes). Based on the general formulation of [9], section 10.4.1, it can be shown that the expected value of $e_{\mathrm{Cone}_l}(\Omega)$ in Eq. (14) in a stochastic angular-rate environment is

$$E(e_{\mathrm{Cone}_l}) = \int_0^{\infty} \dot{\Phi}_{\mathrm{Dens}}(\Omega)\left[2\left(\sum_{s=1}^{N-1} C_s f_s(T_k\Omega)\right) - \left(1 - \frac{\sin(L_{kl}T_k\Omega)}{L_{kl}T_k\Omega}\right)L_{kl}\right]T_k\,\mathrm{d}\Omega \tag{20}$$

where $E(\,)$ is the expected value operator and $\dot{\Phi}_{\mathrm{Dens}}(\Omega)$ is a density function for coning of the sensor assembly such that the expected value of $\dot{\Phi}(\Omega)$ is given by

$$E(\dot{\Phi}) = \int_0^{\infty} \dot{\Phi}_{\mathrm{Dens}}(\Omega)\,\mathrm{d}\Omega \tag{21}$$

Depending on the relative phasing of the correlated angular-rate sensor responses between axes, $\dot{\Phi}_{\mathrm{Dens}}(\Omega)$ will vary in magnitude and polarity as a function of Ω. The relative phasing is not easily predictable, making it difficult to evaluate Eq. (20) analytically.

On a worst-case basis, Eq. (20) can be evaluated by assuming phasing that maximizes the Eq. (20) expected value. Then Eq. (20) with $T_k\Omega = \beta$ becomes

$$E(e_{\text{Cone}_l}) = \int_0^{\infty} \frac{\dot{\Phi}_{\text{DensMax}}(\Omega)}{T_k} \left| 2\left(\sum_{s=1}^{N-1} C_s f_s(\beta)\right) - \left(1 - \frac{\sin(L_{kl}\beta)}{L_{kl}\beta}\right) L_{kl} \right| T_k \, \mathrm{d}\beta \tag{22}$$

An optimum set of C_s coefficients can now be defined as those that minimize $E(e_{\text{Cone}_l})$ in Eq. (22). Because Eq. (22) is nonlinear in C_s, there is no simple analytic method for evaluating the optimum coefficients, thereby requiring a numerical optimization method as a substitute. Alternatively, an analytically definable set of optimum coefficients can be generated as those that minimize the square of the Eq. (22) integrand over a design frequency range. Then the parameter to be minimized is z given by:

$$z = \int_{\beta=0}^{\beta=\beta_{\text{Range}}} \left(\frac{\dot{\Phi}_{\text{DensMax}}(\Omega)}{T_k}\right)^2 \left[2\left(\sum_{s=1}^{N-1} C_s f_s(\beta)\right) - \left(1 - \frac{\sin(L_{kl}\beta)}{L_{kl}\beta}\right) L_{kl} \right]^2 T_k^2 \, \mathrm{d}\beta \tag{23}$$

Comparing Eq. (23) with the Eq. (15) z expression minimized for optimum C_s under discrete inputs, we see that the minimization problems can be made equivalent by equating $\dot{\Phi}(\Omega)$ in Eq. (15) to

$$\dot{\Phi}(\Omega) = \dot{\Phi}_{\text{DensMax}}(\Omega)/T_k \tag{24}$$

With this substitution, the Eqs. (17) and (19) Explicit coefficient formulas can then be used to optimize coefficients for a stochastic angular-rate environment. For confirmation of acceptable results, the computed coefficients should then be tested using the Eq. (22) worst-case formula.

Accommodating Variations in Coning Rates Between Sensor Axes

In the previous development, the Explicit frequency shaping coefficients were computed based on specifying $\dot{\Phi}(\Omega)$. Minimizing Eq. (15) (or Eq. (23)) was then used for algorithm coefficient determination. Note, however, that the rationale leading to Eq. (15) [or Eq. (23)] implicitly assumed the same expected $\dot{\Phi}(\Omega)$ values for each component of the $\delta\underline{\phi}_{\text{Algo}_l}$ coning correction. For a more general development, this constraint is not necessary and can be easily removed, permitting independent frequency shaping for each component of $\delta\underline{\phi}_{\text{Algo}_l}$. The method is to define separate values of $\dot{\Phi}(\Omega)$ for each $\delta\underline{\phi}_{\text{Algo}_l}$ component axis (i.e., $\dot{\Phi}_x(\Omega)$, $\dot{\Phi}_y(\Omega)$, and $\dot{\Phi}_z(\Omega)$), with coefficients then computed separately, exactly as shown previously but for each axis, thereby obtaining C_{x_s}, C_{y_s}, C_{z_s} independent axis coefficients. The C_{x_s}, C_{y_s}, C_{z_s} coefficients would then be applied to compute $\delta\underline{\phi}_{\text{Algo}_l}$ using a revised version of Eq. (8) in which the scalar coefficient C_s is replaced by a three-by-three diagonal square matrix having C_{x_s}, C_{y_s}, C_{z_s} for the diagonal elements.

Specifying Coning Rates for Explicit Coefficient Determination

Explicit frequency shaping can be used in the traditional manner by determining coefficients that minimize the least-squares coning correction error over a uniform magnitude coning versus frequency environment (e.g., for a unity coning rate). The principal advantage for the new Explicit approach, however, is the ability to shape the $\delta\phi_{\text{Algo}_l}$ coning correction to an expected coning environment based on performance specifications for the strapdown system application. Following is generalized analytical methodology for translating system angular rate, acceleration and vibration performance requirements into maximum expected coning conditions. Included is a simple analytical method to account for the effect of sensor assembly vibration isolator dynamics on gyro coning motion inputs. $\dot{\Phi}(\Omega)$ is most conveniently described as a function of coning frequency Ω. As with most frequency based design approaches, Explicit frequency shaping has been formulated using normalized β parameters when determining the A and $\underline{b}$ matrices for coefficient evaluation [i.e., Eq. (20) with Eqs. (13) and (18)]. The Ω frequency in $\dot{\Phi}(\Omega)$ is converted from β to Ω format using the substitution $\Omega = \beta/T_k$.

For Explicit design based on discrete coning rates, $\dot{\Phi}(\Omega)$ can be based on maximum maneuver and vibration limits in the system performance specification. The magnitude of $\dot{\Phi}(\Omega)$ would be of the general Eq. (10) form $\frac{1}{2}\Omega\theta_{0_a}\theta_{0_b}$, with a/b corresponding to x/y, y/z, or z/x for determining $\dot{\Phi}(\Omega)$ along $\delta\underline{\phi}_{\text{Algo}}$ axes z, x, y respectively. Two θ_0 design limits can be considered: 1) a maneuver limit governed by angular rate ω_{Lim} or by angular acceleration ω_{DotLim}, and 2) a vibration limit governed by angular response to an input linear acceleration vibration limit a_{VibLim}. For sinusoidal oscillations at frequency Ω with amplitudes at these limits, the corresponding θ_{0_a}, θ_{0_b} amplitudes would be

$$\theta_{\omega\text{Lim}_a} = \frac{\omega_{\text{Lim}_a}}{\Omega} \qquad \theta_{\omega\text{Lim}_b} = \frac{\omega_{\text{Lim}_b}}{\Omega}$$

$$\theta_{\omega\text{DotLim}_a} = \frac{\omega_{\text{DotLim}_a}}{\Omega^2} \qquad \theta_{\omega\text{DotLim}_b} = \frac{\omega_{\text{DotLim}_b}}{\Omega^2}$$

$$\theta_{\text{VibLim}_a} = H_{\theta_a}(\Omega) a_{\text{VibLim}} \qquad \theta_{\text{VibLim}_b} = H_{\theta_b}(\Omega) a_{\text{VibLim}}$$

where H_{θ_a}, H_{θ_b} are sensor assembly mechanical isolator/mount transfer functions relating gyro angular response around axes a and b to system acceleration input. A generalized $H_\theta(\Omega)$ expression for the $H_{\theta_a}, H_{\theta_b}$ transfer functions is derived in [9], section 10.6.1 based on a simplified model for sensor assembly mount imbalance

$$H_\theta(\Omega) = \frac{1}{D}\sqrt{\frac{\omega_\theta^4(\varepsilon_k + 4\varepsilon_d)^2 + 4\zeta_\theta^2\omega_\theta^2(\varepsilon_c + 4\varepsilon_d)^2\Omega^2}{[(\omega_\theta^2 - \Omega^2)^2 + 4\zeta_\theta^2\omega_\theta^2\Omega^2][(\omega_x^2 - \Omega^2)^2 + 4\zeta_x^2\omega_x^2\Omega^2]}} \tag{25}$$

where ω_x, ζ_x is undamped natural frequency and damping ratio for the sensor-assembly/mount linear vibration motion dynamic response characteristic, $\omega_\theta, \zeta_\theta$ is undamped natural frequency and damping ratio for the sensor-assembly/mount rotary vibration motion dynamic response characteristic, D is the distance between the sensor-assembly mounting points, $\varepsilon_k, \varepsilon_c$ are the sensor-assembly mounting structure spring, damping cross-coupling error coefficients, and ε_d is the distance from the sensor-assembly mount center of force to the sensor assembly center of mass, divided by D. Coning rate amplitude $\dot{\Phi}(\Omega)$ is then equated to $\frac{1}{2}\Omega\theta_{0_a}\theta_{0_b}$ with the θ_{0_a}, θ_{0_b} amplitudes set based on the angular-rate/angular-acceleration or angular vibration limit conditions. For the ω_{Lim} and ω_{DotLim} maneuver limits two versions of $\dot{\Phi}(\Omega)$ can be defined, one with θ_{0_a}, θ_{0_b} set to $\theta_{\omega\text{Lim}_a}, \theta_{\omega\text{Lim}_b}$ and one with $\theta_{0_a}, \theta_{0_b}$ set to $\theta_{\omega\text{DotLim}_b}, \theta_{\omega\text{DotLim}_b}$. The associated $\dot{\Phi}(\Omega)$ values would be $\frac{1}{2}\frac{\omega_{\text{Lim}_a}\omega_{\text{Lim}_b}}{\Omega}$ and $\frac{1}{2}\frac{\omega_{\text{DotLim}_a}\omega_{\text{DotLim}_b}}{\Omega^3}$. A composite maneuver limit $\dot{\Phi}_{\text{MnvrLim}}(\Omega)$ would be equated to the smallest of these. The vibration coning limit would be $\frac{1}{2}\Omega\theta_{0_a}\theta_{0_b}$ with θ_{0_a} and θ_{0_b} set to $H_{\theta_a}(\Omega)a_{\text{VibLim}}$ and $H_{\theta_b}(\Omega)a_{\text{VibLim}}$, or $\dot{\Phi}_{\text{VibLim}}(\Omega) = \frac{1}{2}\Omega H_{\theta_a}(\Omega)H_{\theta_b}(\Omega)a_{\text{VibLim}}^2$. Coning rate $\dot{\Phi}(\Omega)$ is then equated to the largest of $\dot{\Phi}_{\text{MnvrLim}}(\Omega)$ or $\dot{\Phi}_{\text{VibLim}}(\Omega)$.

As an example of the previous procedure, consider the following numerical values for the system design parameters:

$$\omega_{\text{Lim}_a} = 400 \text{ deg/s} \qquad \omega_{\text{Lim}_b} = 180 \text{ deg/s}$$

$$\omega_{\text{DotLim}_a} = 1,080 \text{ deg/s}^2 \qquad \omega_{\text{DotLim}_b} = 360 \text{ deg/s}^2$$

$$a_{\text{VibLim}} = 5 \text{ gs} \tag{26}$$

$$\omega_x = 2\pi \times 50 \text{ Hz} = 100\pi \text{ rad/s} \qquad \varsigma_x = 0.125$$
$$\omega_\theta = \sqrt{2}\omega_x \qquad \varsigma_\theta = \sqrt{2}\varsigma_x \qquad D = 7 \text{ in.}$$
$$\varepsilon_k = 2\% \qquad \varepsilon_c = 2\% \qquad \varepsilon_d = 0.5\% \tag{27}$$

Using Eqs. (26) and (27) with $L_{kl} = 4$ and $H_{\theta_a}(\Omega) = H_{\theta_b}(\omega) = H_\theta(\Omega)$ from Eq. (25), Fig. 1 is a plot of coning rate $\dot{\Phi}(\Omega)$ versus normalized frequency parameter β/π (i.e., β in pi radians) constructed using the previously described procedure. Included is a plot of the coning correction rate $\delta\dot{\phi}(\Omega)$ defined as $\delta\phi_l$ in Eq. (10) divided by T_l:

$$\delta\dot{\phi} = \dot{\Phi}(\Omega)\left(1 - \frac{\sin(\Omega T_l)}{\Omega T_l}\right) \tag{28}$$

For Explicit design based on stochastic environments, $\dot{\Phi}_{\text{DensMax}}(\Omega)/T_k$ for Eq. (24) would be based on coning rates induced on the sensor assembly by random vibration applied to the system. Using the general formulation method of [9], section 10.4.1, it can be shown that $\dot{\Phi}_{\text{Dens}}(\Omega)/T_k$ in Eq. (20) is

$$\dot{\Phi}_{\text{Dens}}(\Omega) = \Omega H_{\theta_a}(\Omega) H_{\theta_b}(\Omega) \sin[\psi_{\theta_a}(\Omega) - \psi_{\theta_b}(\Omega)] G_{a\text{Vib}}(\Omega) \tag{29}$$

where $G_{a\text{vib}}(\Omega)$ is the power spectral density of an applied $a_{\text{Vib}}(t)$ acceleration vibration, and $H_{\theta_a}(\Omega)$, $H_{\theta_b}(\Omega)$, $\psi_{\theta_a}(\Omega)$, $\psi_{\theta_b}(\Omega)$ are angular amplitude and phase angle (Bode type) responses around orthogonal axes $\underline{u}_a$ and $\underline{u}_b$ to an applied unity amplitude sinusoidal linear acceleration input at frequency Ω. It is to be noted that $G_{a\text{Vib}}(\Omega)$ in Eq. (29) is in units of acceleration^2/(rad/s) rather than the more commonly used acceleration^2/Hz so that the variance of $a_{\text{Vib}}(t)$ is given by

$$E(a_{\text{Vib}}(t)^2) = \int_0^\infty G_{a\text{Vib}}(\Omega)\, \mathrm{d}\Omega \tag{30}$$

For worst-case phasing with $H_{\theta_a}(\Omega)$ and $H_{\theta_b}(\Omega)$ equated to $H_\theta(\Omega)$ in Eqs. (25) and (29) with Eq. (21) and the [9], section 10.4.1methodology become

$$\dot{\Phi}_{\text{DensMax}}(\Omega) = \Omega H_\theta(\Omega)^2 G_{a\text{Vib}}(\Omega) \tag{31}$$

$$E(\dot{\Phi}) = \int_0^\infty \frac{\dot{\Phi}_{\text{DensMax}}(\Omega)}{T_k}\, \mathrm{d}\beta \tag{32}$$

The worst-case expected value of the coning correction rate $E(\delta\dot{\phi})$ is evaluated similarly

$$E(\delta\dot{\phi}) = \int_0^\infty \left|\frac{\delta\dot{\phi}_{\text{DensMax}}(\Omega)}{T_k}\right| \mathrm{d}\beta \tag{33}$$

where by extension of Eq. (28)

$$\delta\dot{\phi}_{\text{DensMax}}(\Omega) = \dot{\Phi}_{\text{DensMax}}(\Omega)\left|1 - \frac{\sin(L_{kl}\beta)}{L_{kl}\beta}\right| \tag{34}$$

As an example of the previous procedure, consider $G_{a\text{Vib}}(\Omega)$ being modeled as 0 from $\Omega = 0$ to 80 rad/s, increasing exponentially from 0.00159 to 0.00637 g^2 per rad/s (i.e., 0.01 to 0.04 g^2/Hz) over 80 to 120 rad/s, sustaining 0.00637 g^2 per rad/s from 120–6, 000 rad/s, decreasing exponentially to 0.00159 g^2 per rad/s over 6000 to 12, 000 rad/s, and being 0 thereafter. Using Eq. (30), this corresponds to an rms input vibration acceleration $\sqrt{E(a_{\text{Vib}}(t)^2)}$ of 7.63 gs. For $T_k = 0.001$ s and $H_\theta(\Omega)$ from Eq. (25) using the Eq. (27) numerical parameters, Fig. 2 describes $\dot{\Phi}_{\text{DensMax}}/T_k$ and absolute $\delta\dot{\phi}_{\text{DensMax}}/T_k$ from Eqs. (31) and (39) with $L_{kl} = 4$ as a function of normalized frequency β in pirads (β/π). Using Eqs. (32) and (33) with Eqs. (31) and (34), the corresponding worst-case expected total attitude coning rate $E(\dot{\Phi})$ is 1.38 deg /h with an expected coning correction rate $E(\delta\dot{\phi})$ of 0.404 deg /h.

Evaluating Coning Algorithm Performance

Coning correction algorithm performance was evaluated for the paper under discrete and stochastic coning conditions, and for an extreme dynamic maneuver. The analytical methods used for each are described next.

Algorithm performance in a discrete coning environment was evaluated as the average error buildup rate $\dot{e}_{\text{Cone}}(\Omega)$ defined as $e_{\text{Cone}_l}(\Omega)$ in Eq. (10) divided by T_l

$$\dot{e}_{\text{Cone}}(\Omega) = \dot{\Phi}_{\text{Eval}}(\Omega)\left[\frac{2}{L_{kl}}\left(\sum_{s=1}^{N-1} C_s f_s(\beta)\right) - \left(1 - \frac{\sin(L_{kl}\beta)}{L_{kl}\beta}\right)\right] \tag{35}$$

where $\dot{\Phi}_{\text{Eval}}(\Omega)$ is the total attitude coning rate used for performance evaluation (as contrasted with $\dot{\Phi}(\Omega)$ used for Explicit algorithm coefficient design). The Eval notation in Eq. (35) allows for differences in coning rate values used for performance evaluation and coefficient determination. Note that for a traditional normalized type error evaluation (e.g., [7,8]), $\dot{\Phi}_{\text{Eval}}(\Omega)$ would be set to unity for all Ω.

In a stochastic coning environment, the expected algorithm error rate $E(\dot{e}_{\text{Cone}})$, the expected total attitude coning rate $E(\dot{\Phi})$, and the expected coning correction rate $E(\delta\dot{\phi})$ were evaluated similarly based on Eqs. (22) and (32–34) as

$$E(\dot{e}_{\text{Cone}}) = \int_0^\infty \left|\frac{2}{L_{kl}}\frac{\dot{\Phi}_{\text{DensMax/Eval}}(\Omega)}{T_k}\left(\sum_{s=1}^{N-1} C_s f_s(\beta)\right) - \frac{\delta\dot{\phi}_{\text{DensMax/Eval}}(\Omega)}{T_k}\right| \mathrm{d}\beta \tag{36}$$

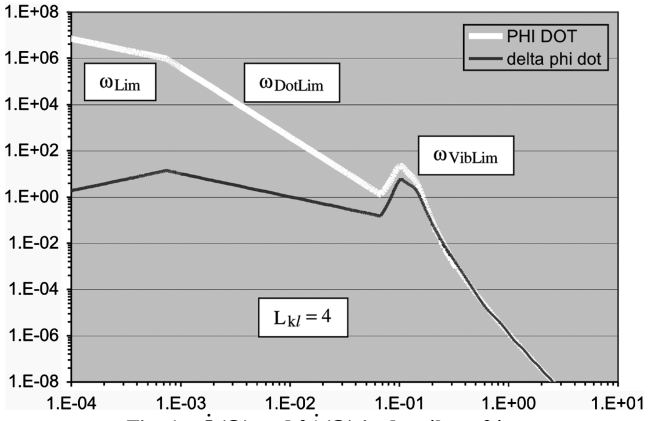

Fig. 1 $\dot{\Phi}(\Omega)$ and $\delta\dot{\phi}(\Omega)$ in deg /h vs β/π.

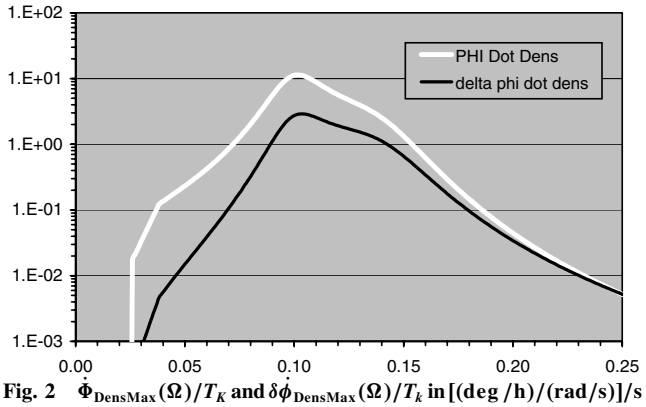

Fig. 2 $\dot{\Phi}_{\text{DensMax}}(\Omega)/T_K$ and $\delta\dot{\phi}_{\text{DensMax}}(\Omega)/T_k$ in [(deg /h)/(rad/s)]/s vs β/π.

$$E(\dot{\Phi}) = \int_0^{\infty} \frac{\dot{\Phi}_{\text{DensMax/Eval}}(\Omega)}{T_k}\, \mathrm{d}\beta \tag{37}$$

$$E(\delta\dot{\phi}) = \int_0^{\infty} \left| \frac{\delta\dot{\phi}_{\text{DensMax/Eval}}(\Omega)}{T_k} \right| \mathrm{d}\beta \tag{38}$$

$$\delta\dot{\phi}_{\text{DensMax/Eval}}(\Omega) = \dot{\Phi}_{\text{DensMax/Eval}}(\Omega) \left| 1 - \frac{\sin(L_{kl}\beta)}{L_{kl}\beta} \right| \tag{39}$$

In a maneuvering environment, the algorithm error was evaluated as the net attitude error induced by the maneuver (as contrasted with attitude error rate described previously for evaluating performance in a sustained coning environment). Maneuver induced attitude error $e_{\text{Mnvr}}(t)$ was calculated as

$$e_{\text{Mnvr}}(t) =$$

$$\text{Magnitude of Rotation Vector Equivalent to } C_{\text{Algo}}(t)[C_{\text{True}}(t)]^T \tag{40}$$

where $C_{\text{True}}(t)$ is the true direction cosine attitude matrix at time t in the maneuver and $C_{\text{Algo}}(t)$ is the Eq. (1) computed direction cosine matrix at time t using the algorithm under investigation (both initialized at identity). The rotation vector equivalent referred to in Eq. (40) represents the error in $C_{\text{Algo}}(t)$ compared with $C_{\text{True}}(t)$, calculated using a direction-cosine-matrix-to-rotation-vector extraction formula such as described in [9], section 3.2.2.2. For the paper, a $C_{\text{True}}(t)$ solution was obtained by processing a parallel implementation of Eq. (1) updated at a 10 MHz update rate with the rotation vector over each 0.1 μ sec update period approximated as the integrated maneuver angular-rate (i.e., setting the Eq. (2) coning correction to zero as negligible for this update rate). The composite attitude error recorded for each algorithm investigated was the maximum $e_{\text{Mnvr}}(t)$ attitude error experienced over the selected maneuver period. The maneuver chosen for performance evaluation was the extreme 2 s angular-rate/angular-acceleration profile depicted in Fig. 3 based loosely on the Eq. (26) performance parameters. The maximum rotation vector magnitude over the 2 s maneuver (extracted from $C_{\text{True}}(t)$) was 180 deg occurring at 1.55 s.

Algorithm Performance Evaluation Results

To illustrate the characteristics of Explicit compared with time-series and frequency-series designed coning correction algorithms, numerical performance figures were generated for discrete and random coning environments, and under maneuver conditions. Four coning correction algorithm coefficient configurations were evaluated, each with $N = 4$ (four sequential $\Delta\underline{\alpha}$ samples in the $\delta\underline{\phi}_{\text{Algo}_l}$ calculation), $L_{kl} = N$ (coning correction computation rate N times slower than the sensor sampling rate such that all $\Delta\underline{\alpha}$ samples for coefficient determination are contained within the current l cycle), and $T_k = 0.001$ s (1 KHz sensor sampling rate corresponding to 20 times 50 Hz, the assumed Eq. (27) linear vibration mode undamped natural frequency $\omega_x/2\pi$ for the sensor assembly mount):

1) XplDscrt- Uses Explicit (Xpl) coefficients designed for discrete (Dscrt) coning environments.

2) XplRnd- Uses Explicit (Xpl) coefficients designed for random (Rnd) environments.

3) FSr- Uses Appendix B frequency-series designed coefficients.

4) TSr- Uses Appendix A time-series designed coefficients.

Two baseline references were also generated for algorithm performance comparisons: 1) Bas-00, with sensor errors but using an exact attitude updating algorithm (i.e., no algorithm error), and 2) Bas-01, using Eqs. (1) and (2) for attitude updating but without $\delta\underline{\phi}_{\text{Algo}_l}$ coning correction. Bas-00 was created using sensor input data containing 5 μrad misalignment and 5 ppm scale factor error for each sensor assembly axis (representative of a typical well calibrated aircraft INS). The exact algorithm for Bas-00 was formed as a parallel computation of the $C_{\text{True}}(t)$ truth model described in the previous section.

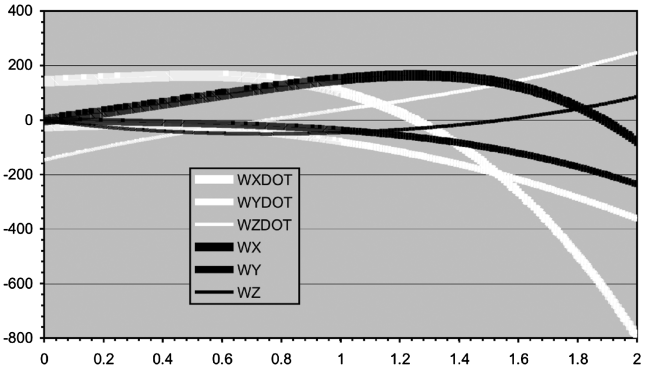

Fig. 3 Angular rate (deg /s) and angular acceleration (deg /s^2) vs time (s).

For Explicit algorithm coefficient determination, β_{Range} was set to π, $\dot{\Phi}(\Omega)$ was set to the Fig. 1 values, and $\dot{\Phi}_{\text{DensMax}}(\Omega)/T_k$ was set to the Fig. 2 values.

Coefficients and accuracies for the four coning correction algorithms are presented in Tables 1 and 2. The random environment error in Table 2 is $E(\dot{e}_{\text{Cone}})$ from Eq. (36) using Fig. 2 for the $\dot{\Phi}_{\text{DensMax/Eval}}(\Omega)/T_k$ coning rate density; the maneuver error is the maximum of $e_{\text{Mnvr}}(t)$ from Eq. (40) over the Fig. 3 maneuver profile. The Bas-00 random environment error in Table 2 was calculated from formulas provided in [9], sections 8.2.1.1 and 10.4.1.

Figure 4 presents absolute value plots of algorithm error $\dot{e}_{\text{Cone}}(\Omega)$ in a discrete coning environment using Eq. (35) and Fig. 1 for the $\dot{\Phi}_{\text{Eval}}(\Omega)$ coning rate profile. To simplify Fig. 4, discrete error plots for the Bas-00 and Bas-01 reference cases have not been included. Using [9], section 8.2.1.1, the Bas-00 discrete error equals $\dot{\Phi}(\Omega)$ from Fig. 1 multiplied by 1.E-5, the root-sum-squared composite of misalignments for the sensor along the coning axis and scale factor error for the sensors orthogonal to the coning axis. The Bas-01 discrete error equals $\delta\dot{\phi}(\Omega)$ in Fig. 1. At $\beta/\pi = 0$, all error plots in Fig. 4 are zero (off scale in the figure). The peak value of XplRnd in Fig. 4 is $8.05\text{E}-5$ deg /h occurring off scale at $\beta/\pi = 7.04\text{E}-4$ (the ω_{Lim} to ω_{DotLim} breakpoint in Fig. 1). Figure 5 is the normalized

Table 1 Coning correction algorithm coefficients ($L_{kl} = 4$)

Coning algorithm	C1	C2	C3
Bas-00	N/a	N/a	N/a
Bas-01	0	0	0
XplDscrt	2.045	0.8709	0.5156
XplRnd	2.050	0.8663	0.5169
FSr	2.038	0.8762	0.5143
TSr	2.250	0.7069	0.5566

Table 2 Coning correction algorithm errors in random and maneuver environments ($L_{kl} = 4$)

Coning correction algorithm	Random coning environment error, deg /h	Maximum maneuver error, μrad
Bas-00	1.38E-5	21.3
Bas-01	4.04E-1	17.4
XplDscrt	2.75E-6	0.0249
XplRnd	2.55E-6	0.0250
FSr	4.06E-6	0.0249
TSr	8.69E-5	0.0253[a]
		0.000178[b]

[a]With compressed Eq. (8) coefficients.
[b]With uncompressed Eq. (5) coefficients.

equivalent to Fig. 4 obtained with Table 1 coefficients by setting $\dot{\Phi}_{\text{Eval}}(\Omega)$ in Eq. (35) to unity.

In Table 1, the Time-series coefficients are the Eq. (9) compressed equivalent version of the full Eq. (5) coefficient matrix ς_{ij} that would effectively exist in a coning environment (and are the values used for time-series algorithm coning environment performance evaluation). In Table 2, two values are shown for the time-series maneuver error, one using the Table 1 compressed coefficients with algorithm Eq. (8) during the Fig. 3 maneuver, the other using uncompressed ς_{ij} matrix coefficients with algorithm Eq. (5).

Note in Table 2 that the maneuver error for Bas-00 (exact attitude updating with sensor errors) is 21.3 μrad; the maneuver error for Bas-01 (perfect sensors using a standard attitude algorithm but without coning correction) is 17.4 μrad (i.e., comparable to Bas-00). These points illustrate that for 1 KHz sensor sampling with 250 Hz attitude updating ($L_{kl} = 4$) in Table 2, coning effects produced under maneuvers can have a significant impact on system performance, hence, should not be ignored when designing coning correction computation algorithms. Also note in Table 2 that the TSr algorithm with full uncompressed coefficients has 2 orders of magnitude smaller maneuvering error than the equivalent TSr algorithm with compressed coefficients. However, the compressed TSr and frequency based algorithms (Xpl and FSr) still have negligible error (by almost 2 orders of magnitude) compared with Bas-00 or Bas-01. These points illustrate (as analytically shown in [7,8]) that designing algorithms for optimum pure coning performance (Xpl and FSr) introduces negligible performance penalty when operated in maneuvering environments.

Comparing algorithm errors under random environments, Table 2 shows that the performance for Explicit algorithm designed coefficients (XplRnd and XplDscrt) is superior to the others tested. Figure 4 illustrates the balanced accuracy versus frequency characteristic of the Explicit compared with the equivalent frequency-series and time-series algorithms (XplDscrt or XplRnd vs FSr and TSr). The FSr and TSr algorithms sacrifice midfrequency performance for high accuracy at lower frequencies. In contrast, the Explicit algorithms achieve balanced performance across the frequency range. Similar conclusions can be drawn from the Fig. 5 normalized performance curves for the Fig. 1 coning profile (the evaluation basis for Fig. 4). Note also in Figs. 4 and 5 that the XplDscrt algorithm (designed to handle Fig. 1 increasing coning magnitude at low frequencies) has superior low-frequency accuracy compared with XplRnd designed for Fig. 2 coning with no low-frequency coning content.

Parameter Variations

An important part of coning correction algorithm design is selection of the key performance parameters associated with coefficient determination. For all algorithms, the sensor sampling time interval

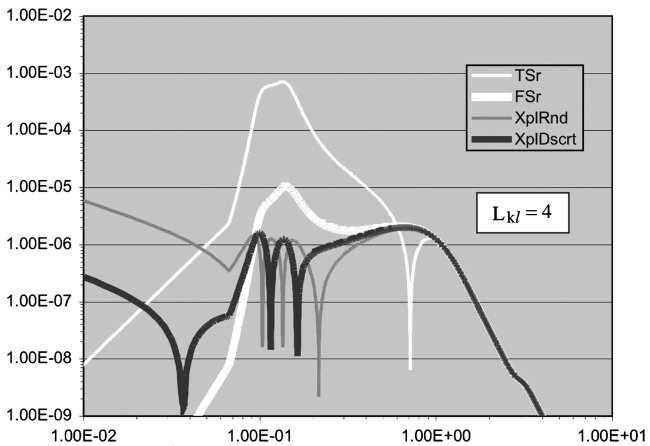

Fig. 4 Discrete $\dot{\Phi}(\Omega)$ weighted coning correction algorithm error (deg /h) vs β/π.

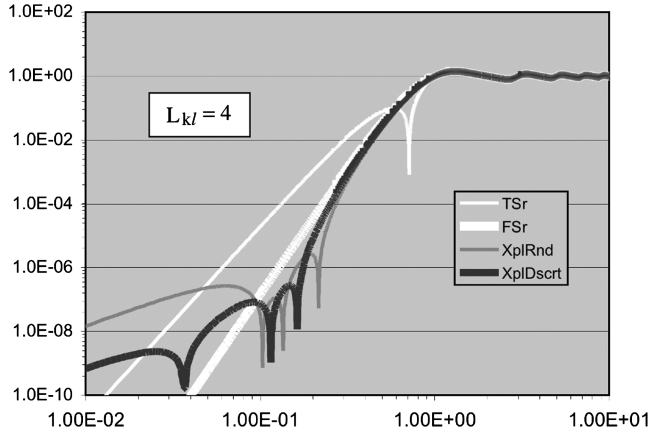

Fig. 5 Discrete normalized coning correction algorithm error vs β/π.

T_k is critical to assure that it is small enough to accurately measure expected $\dot{\Phi}(\Omega)$ coning effects. For the examples cited, T_k was set to 0.001 s (i.e., 1 KHz), 20 times the 50 Hz resonance frequency of the assumed sensor assembly isolation configuration. For the Explicit approach, this provided a fundamental $f_s(\beta)$ mode [i.e., $s = 1$ in Eq. (11)] having a smooth nonzero amplitude shape over the frequency range of the coning correction profile being fitted, plus two higher harmonic $f_s(\beta)$ modes ($s = 2$ and 3) to shape the algorithm response; see Eq. (11). Note that each $f_s(\beta)$ harmonic has a nodal (zero) point for $\beta = \pi/s$. This is somewhat analogous to selection of the fundamental harmonic frequency when fitting a truncated Fourier series to a time function. The β_{Range} parameter was set to π for similar reasons. Larger T_k values created too much curvature for the $f_s(\beta)$ mode shapes over the coning frequencies being fitted resulting in poorer performance (or requiring more $f_s(\beta)$ higher frequency mode shapes to recover accuracy, i.e., more sensor samples N in the coning algorithm). Smaller T_k values (higher sensor sampling rate) improved accuracy significantly, but only when accompanied by larger N (more high frequency $f_s(\beta)$ components) to fit the reduced β frequency range of the Fig. 1 coning profile (i.e., for smaller T_k, $\beta = \Omega T_k$ is smaller for a given Ω). More complex coning rate profiles generally require more sensor samples in the coning algorithm for best results.

To illustrate the potential impact of too large a T_k value, test cases were rerun with T_k increased to 0.002 s (two times larger than used in Fig. 4). Results significantly increased the TSr, FSr, XplDscrt algorithm vibration resonance error peaks in Fig. 4 to 0.0348 deg /h, 0.00229 deg /h and 0.000255 deg /h, respectively. Compared with a 0.01 deg /h gyro accuracy requirement for a typical aircraft INS, it could be concluded that a 0.002 s T_k setting is unacceptable for a TSr algorithm and marginal for an FSr algorithm. The comfortable XplDscrt algorithm design margin indicated in this case would provide a reserve to handle potential off-nominal coning conditions. When the number of gyro samples N in the XplDscrt algorithm was increased from four to six (including an L_{kl} increase to six), the 0.000255 deg /h XplDscrt resonance error peak decreased by an order of magnitude (to 0.0000275 deg /h).

To illustrate the effect of a smaller value for T_k than needed, test cases were run with T_k reduced by a factor of 10 (to 0.0001 s). For $N = L_{kl} = 4$ as in Fig. 4, the XplDscrt vibration resonance error peak was reduced by a factor of 2.8. For $N = L_{kl} = 10$, the XplDscrt resonance error peak was reduced by a factor of 52.

The L_{kl} parameter was set to four for the $N = 4$ (four sensor sample) cases cited to match previous algorithms described in [7,8]. Smaller values could be used if a faster attitude computation rate is desired. (Note that slower attitude computation rate for the same accuracy can be obtained for given N, L_{kl}, T_k settings using the two-speed Eq. (3) attitude updating approach.) Decreasing L_{kl} significantly decreased the maneuver error in Table 2 for all algorithms (e.g., by 35 times for XplDscrt). However, for the Explicit and frequency-series algorithms, the error in coning environments (random in Table 2 and discrete in Fig. 4) was unchanged for

decreased L_{kl}. Curiously, the Table 2 and Fig. 4 time-series algorithm coning error increased for decreased L_{kl}. For example, for coefficients calculated with $L_{kl} = 1$, the time-series algorithm error increased by 2.3 times over the Table 2 random coning and Fig. 4 discrete coning performance values.

When designing Explicit coefficients for a traditional uniform (constant) coning environment, it is important that β_{Range} be set to only cover the frequency range over which $\dot{\Phi}(\Omega)$ coning inputs are expected (e.g., for the Fig. 1 coning environment, setting β_{Range}/π to 0.2). Larger β_{Range}/π values give weighting to higher frequency nonconing regions at sacrifice of low-frequency performance.

Cautionary Note

Numerical matrix inversion was used to compute algorithm coefficients presented in this paper. In some unusual cases, numerical roundoff impacted Explicit results obtained (e.g., for $N > 6$ or with the sensor sample rate T_k set to 0.0001 s, 10 times higher than needed for the Fig. 1 coning profile). A simple solution was to provide a very small artificial lower limit to $\dot{\Phi}(\Omega)$ in Fig. 1 so that its value never approached zero (for the previous examples the limit was set to 0.000001 deg/h, well below the 0.01 deg/h gyro accuracy requirement for a typical aircraft INS). (This is analogous to adding artificial measurement noise in a Kalman filter optimal gain calculation to avoid numerical matrix inversion singularities.) It is recommended when computing coefficients that the matrix inversion routine be tested for accuracy by pre and postmultiplying its output with the matrix being inverted to assure that the result (call it I^*) equals identity within acceptable limits (e.g., so that each element of I^* is within 2.E-6 of the correct identity matrix value).

Conclusions

Explicit frequency shaping is an effective method for structuring strapdown coning correction algorithms for accurate response in expected discrete or stochastic coning environments. Algorithm accuracy in maneuver environments exceeds requirements for a typical aircraft high performance INS. Accuracy is improved over previous Taylor series expansion designed algorithms in expected (or uniform) coning amplitude versus frequency profiles. Explicit frequency shaping allows optimization for user specified coning versus frequency environments and can be independently tailored for each computation axis. Using the methods provided in the paper, system performance requirements are easily translated into expected discrete or random coning versus frequency values for Explicit coefficient determination. The Explicit method can also be used in the traditional sense for coefficient design based on a uniform (constant) coning amplitude versus frequency profile. Some numerical experimentation is generally required for Explicit parameter selection to achieve the best results.

Appendix A: Time-Series Coning Correction Algorithm Coefficients

This appendix derives a general equation for calculating $\delta\underline{\phi}$ coning correction algorithm coefficients based on Taylor series expansion in time t for angular rate $\underline{\omega}$ around a general time point t_0.

For an Nth order Taylor series

$$\underline{\omega}(t) = \underline{\omega}(t_0) + \sum_{i=2}^{N}\left(\frac{\mathrm{d}^{i-1}}{\mathrm{d}t^{i-1}}\underline{\omega}(t)_{t=t_0}\right)\frac{1}{(i-1)!}(t-t_0)^{i-1} = \underline{\omega}(\tau)$$
$$= \underline{\omega}(\tau=0) + \sum_{i=2}^{N}\left(\frac{\mathrm{d}^{i-1}}{\mathrm{d}\tau^{i-1}}\underline{\omega}(\tau)_{\tau=0}\right)\frac{1}{(i-1)!}\tau^{i-1} \tag{A1}$$

where τ is time relative to t_0, i.e., $\tau \equiv t - t_0$. Equivalently

$$\underline{\omega}(\tau) = \sum_{i=1}^{N}\underline{b}_i\tau^{i-1} \qquad \underline{b}_i = \left(\frac{\mathrm{d}^{i-1}}{\mathrm{d}\tau^{i-1}}\underline{\omega}(\tau)_{\tau=0}\right)\frac{1}{(i-1)!}$$
$$\underline{b}_1 = \underline{\omega}(\tau=0) \tag{A2}$$

From Eq. (A2), the jth integrated angular-rate sample for algorithm input is for an integration sample time interval $\Delta\tau_j$ ending at time τ_j

$$\Delta\underline{\alpha}_j = \int_{\tau_j-\Delta\tau_j}^{\tau_j}\underline{\omega}(\tau)\,\mathrm{d}\tau = \sum_{i=1}^{N}\left[\frac{1}{i}\left(\tau_j^i - (\tau_j-\Delta\tau_j)^i\right)\underline{b}_i\right] \tag{A3}$$

or equivalently

$$\Delta\underline{\alpha}_j = \sum_{i=1}^{N}\lambda_{ji}\underline{b}_i \qquad \lambda_{ji} \equiv \frac{1}{i}\left(\tau_j^i - (\tau_j-\Delta\tau_j)^i\right) \tag{A4}$$

The transpose of Eq. (A4) is

$$\Delta\underline{\alpha}_j^T = \sum_{i=1}^{N}\lambda_{ji}\underline{b}_i^T \tag{A5}$$

or in matrix form

$$\Delta A = \Gamma B \tag{A6}$$

where ΔA is the matrix whose rows are the $\Delta\underline{\alpha}_j^T s$ from $j = 1$ to N, B is the matrix whose rows are the $\underline{b}_i^T s$ from $i = 1$ to N, and Γ is the matrix whose j rows i columns are the $\lambda_{ji}s$.

Solving for B from Eq. (A6) then gives $B = \Gamma^{-1}\Delta A$ or equivalently

$$\underline{b}_i = \sum_{j=1}^{N}\kappa_{ij}\Delta\underline{\alpha}_j \tag{A7}$$

where κ_{ij} is the element in row i column j of Γ^{-1}. Equation (A7) shows that each $\underline{b}_i$ can be formed as a linear weighted sum of $\Delta\underline{\alpha}_j s$, and that the integration time interval and end time for each $\Delta\underline{\alpha}_j$ is completely independent from any other $\Delta\underline{\alpha}_j$.

Now consider the coning correction integral $\delta\underline{\phi}_l$ which, from Eq. (2), is of the form

$$\delta\underline{\phi}_l = \int_{t_{l-1}}^{t_l}\frac{1}{2}\underline{\alpha}(t-t_{l-1})\times\mathrm{d}\underline{\alpha} = \int_{t_{l-1}}^{t_l}\frac{1}{2}\underline{\alpha}(t-t_{l-1})\times\underline{\omega}(t)\,\mathrm{d}t$$
$$= \int_{\tau_{l-1}}^{\tau_l}\frac{1}{2}\underline{\alpha}(\tau-\tau_{l-1})\times\underline{\omega}(\tau)\,\mathrm{d}\tau \quad \text{with}$$
$$\underline{\alpha}(\tau-\tau_{l-1}) = \int_{\tau_{l-1}}^{\tau}\mathrm{d}\underline{\alpha} = \int_{\tau_{l-1}}^{\tau}\underline{\omega}(t)\,\mathrm{d}t = \int_{\tau_{l-1}}^{\tau}\underline{\omega}(\tau)\,\mathrm{d}\tau \tag{A8}$$

Substituting for $\underline{\omega}(\tau)$ from Eqs. A2 and A7 finds

$$\underline{\omega}(\tau) = \sum_{p=1}^{N}\underline{b}_p\tau^p = \sum_{p=1}^{N}\left[\left(\sum_{i=1}^{N}\kappa_{pi}\Delta\underline{\alpha}_i\right)\tau^{p-1}\right]$$
$$\underline{\alpha}(\tau-\tau_{l-1}) = \int_{\tau_{l-1}}^{\tau}\underline{\omega}(\tau)\,\mathrm{d}\tau = \sum_{p=1}^{N+1}\left[\frac{1}{p}\left(\sum_{i=1}^{N+1}\kappa_{pi}\Delta\underline{\alpha}_i\right)(\tau^p - \tau_{l-1}^p)\right]$$
$$\underline{\alpha}(\tau-\tau_{l-1})\times\underline{\omega}(\tau) = \left\langle\sum_{p=1}^{N}\left[\frac{1}{p}\left(\sum_{i=1}^{N}\kappa_{pi}\Delta\underline{\alpha}_i\right)(\tau^p-\tau_{l-1}^p)\right]\right\rangle$$
$$\times\sum_{q=1}^{N}\left[\left(\sum_{j=1}^{N}\kappa_{qj}\Delta\underline{\alpha}_j\right)\tau^{q-1}\right]$$
$$= \sum_{p=1}^{N}\sum_{i=1}^{N}\sum_{q=1}^{N}\sum_{j=1}^{N}\frac{1}{p}\kappa_{pi}\kappa_{qj}(\tau^{p+q-1} - \tau_{l-1}^p\tau^{q-1})\Delta\underline{\alpha}_i\times\Delta\underline{\alpha}_j$$
$$= \sum_{j=1}^{N}\sum_{i=1}^{N}\sum_{p=1}^{N}\sum_{q=1}^{N}\frac{1}{p}\kappa_{pi}\kappa_{qj}(\tau^{p+q-1} - \tau_{l-1}^p\tau^{q-1})\Delta\underline{\alpha}_i\times\Delta\underline{\alpha}_j \tag{A9}$$

Substituting $\underline{\alpha}(\tau-\tau_{l-1})\times\underline{\omega}(\tau)$ from Eq. A9 in Eq. A8 then gives

$$\begin{aligned}\delta\underline{\phi}_l &= \int_{\tau_{l-1}}^{\tau_l}\frac{1}{2}\underline{\alpha}(\tau-\tau_{l-1})\times\underline{\omega}(\tau)\,\mathrm{d}\tau \\ &= \sum_{j=1}^{N}\sum_{i=1}^{N}\left\{\sum_{p=1}^{N}\sum_{q=1}^{N}\frac{1}{2}\kappa_{pi}\kappa_{qj}\frac{1}{p}\left[\frac{1}{p+q}(\tau_l^{p+q}-\tau_{l-1}^{p+q})\right.\right. \\ &\quad \left.\left.-\frac{1}{q}\tau_{l-1}^{p}(\tau_l^{q}-\tau_{l-1}^{q})\right]\right\}\Delta\underline{\alpha}_i\times\Delta\underline{\alpha}_j \qquad \text{(A10)}\end{aligned}$$

Recognizing that $\Delta\underline{\alpha}_i\times\Delta\underline{\alpha}_i=0$ and $\Delta\underline{\alpha}_i\times\Delta\underline{\alpha}_j=-\Delta\underline{\alpha}_j\times\Delta\underline{\alpha}_i$, Eq. A10 becomes a final form

$$\begin{aligned}\delta\underline{\phi}_l &= \sum_{j=1}^{N-1}\sum_{i=j+1}^{N}\varsigma_{ij}\Delta\underline{\alpha}_i\times\Delta\underline{\alpha}_j \\ \varsigma_{ij} &= \sum_{p=1}^{N}\sum_{q=1}^{N}\frac{1}{2}(\kappa_{pi}\kappa_{qj}-\kappa_{pj}\kappa_{qi})\frac{1}{p}\left[\frac{1}{p+q}(\tau_l^{p+q}-\tau_{l-1}^{p+q})\right. \\ &\quad \left.-\frac{1}{q}\tau_{l-1}^{p}(\tau_l^{q}-\tau_{l-1}^{q})\right] \qquad \text{(A11)}\end{aligned}$$

Normally the $\Delta\underline{\alpha}s$ are all T_k wide and spaced sequentially backward in time from 1 to N. For $t_0\equiv t_{l-1}$, $\Delta\underline{\alpha}_1$ ends at $t=t_l=t_{l-1}+T_l=t_{l-1}+L_{kl}T_k$, hence, $\Delta\underline{\alpha}_j$ ends at $t=t_{l-1}+L_{kl}T_k-(j-1)T_k=t_{l-1}+(L_{kl}+1-j)T_k$. Then $\tau_j=(L_{kl}+1-j)T_k$, $\Delta\tau_j=T_k$, and $\tau_j-\Delta\tau_j=(L_{kl}+1-j)T_k-T_k=(L_{kl}-j)T_k$. Substituting, λ_{ji} in Eq. A4 then becomes

$$\lambda_{ji}=\frac{1}{i}\left([(L_{kl}+1-j)T_k]^i-[(L_{kl}-j)T_k]^i\right) \qquad \text{(A12)}$$

With $t_0=t_{l-1}$ we also get $\tau_{l-1}=0$ and $\tau_l=T_l=L_{kl}T_k$, so that ς_{ij} in Eq. A11 simplifies to

$$\varsigma_{ij}=\sum_{p=1}^{N}\sum_{q=1}^{N}\frac{\kappa_{pi}\kappa_{qj}-\kappa_{pj}\kappa_{qi}}{2p(p+q)}(L_{kl}T_k)^{p+q} \qquad \text{(A13)}$$

The revised version for the Eq. A11 coning correction algorithm is then given by

$$\delta\underline{\phi}_l=\sum_{j=1}^{N-1}\sum_{i=j+1}^{N}\varsigma_{ij}\Delta\underline{\alpha}_{k+1-i}\times\Delta\underline{\alpha}_{k+1-j} \qquad \text{(A14)}$$

where k is the sample time index for $\Delta\underline{\alpha}$ sampling.

Appendix B: Frequency-Series Coning Correction Algorithm Coefficients

This appendix derives a general equation for calculating $\delta\underline{\phi}$ coning correction algorithm coefficients based on a Miller/Ignagni-type [6–8] Taylor series expansion in powers of normalized coning frequency β.

Frequency-series expansion algorithm coefficients are designed to null error Eq. (14) with Eq. (11). Recognizing in general that

$$\frac{\sin\chi}{\chi}=1-\frac{\chi^2}{3!}+\frac{\chi^4}{5!}-\frac{\chi^6}{7!}+\ldots\approx\sum_{r=1}^{M}\frac{(-1)^{r-1}}{(2r-1)!}\chi^{2(r-1)} \qquad \text{(B1)}$$

where M is the number of terms carried in the series expansion, $f_s(\beta)$ in Eq. (11) becomes

$$\begin{aligned}f_s(\beta) &= \sum_{r=1}^{M}\left[2s\frac{(-1)^{r-1}}{(2r-1)!}(s\beta)^{2(r-1)}-(s-1)\frac{(-1)^{r-1}}{(2r-1)!}[(s-1)\beta]^{2(r-1)}\right. \\ &\quad \left.-(s+1)\frac{(-1)^{r-1}}{(2r-1)!}[(s+1)\beta]^{2(r-1)}\right] \\ &= \sum_{r=1}^{M}[2s^{2r-1}-(s-1)^{2r-1}-(s+1)^{2r-1}]\frac{(-1)^{r-1}}{(2r-1)!}\beta^{2(r-1)} \qquad \text{(B2)}\end{aligned}$$

Because $2s-(s-1)-(s+1)=0$, Eq. (B2) simplifies to

$$f_s(\beta)=\sum_{r=2}^{M}[2s^{2r-1}-(s-1)^{2r-1}-(s+1)^{2r-1}]\frac{(-1)^{r-1}}{(2r-1)!}\beta^{2(r-1)} \qquad \text{(B3)}$$

Setting $r=p+1$ gives $2r-1=2p+1$ and $2(r-1)=2p$ with p limits from 1 to $M-1$. Equation (B3) then becomes

$$f_s(\beta)=\sum_{p=1}^{M-1}[2s^{2p+1}-(s-1)^{2p+1}-(s+1)^{2p+1}]\frac{(-1)^{p}}{(2p+1)!}\beta^{2p} \qquad \text{(B4)}$$

Similarly, the $(1-\frac{\sin(L_{kl}\beta)}{L_{kl}\beta})$ term in Eq. (14) becomes with Eq. (B1)

$$\begin{aligned}1-\frac{\sin(L_{kl}\beta)}{L_{kl}\beta} &= 1-\sum_{r=1}^{M}\frac{(-1)^{r-1}}{(2r-1)!}(L_{kl}\beta)^{2(r-1)} \\ &= -\sum_{r=2}^{M}\frac{(-1)^{r-1}}{(2r-1)!}(L_{kl}\beta)^{2(r-1)} \\ &= -\sum_{r=2}^{M}\frac{(-1)^{r-1}}{(2r-1)!}L_{kl}^{2(r-1)}\beta^{2(r-1)} \\ &= -\sum_{p=1}^{M-1}L_{kl}^{2p}\frac{(-1)^{p}}{(2p+1)!}\beta^{2p} \qquad \text{(B5)}\end{aligned}$$

Substituting Eqs. (B6) and (B7) into Eq. (14) and setting $e_{\mathrm{Algo}_i}(\Omega)$ to zero, then gives with rearrangement

$$\begin{aligned}&(1/L_{kl})\sum_{s=1}^{N-1}\sum_{p=1}^{M-1}2\left(2s^{2p+1}-(s-1)^{2p+1}\right. \\ &\quad \left.-(s+1)^{2p+1}\right)C_s\frac{(-1)^{p}}{(2p+1)!}\beta^{2p} \\ &= \sum_{p=1}^{M-1}\left[\sum_{s=1}^{N-1}2\left(2s^{2p+1}-(s-1)^{2p+1}\right.\right. \\ &\quad \left.\left.-(s+1)^{2p+1}\right)L_{kl}^{-1}C_s\right]\frac{(-1)^{p}}{(2p+1)!}\beta^{2p} \\ &= -\sum_{p=1}^{M-1}L_{kl}^{2p}\frac{(-1)^{p}}{(2p+1)!}\beta^{2p} \qquad \text{(B6)}\end{aligned}$$

Because Eq. (B6) is valid for any β, the coefficients of like powers of β must be equal, hence

$$\sum_{s=1}^{N-1}2\left(2s^{2p+1}-(s-1)^{2p+1}-(s+1)^{2p+1}\right)L_{kl}^{-1}C_s=-L_{kl}^{2p} \qquad \text{(B7)}$$

or

$$\sum_{s=1}^{N-1}2\left(2s^{2p+1}-(s-1)^{2p+1}-(s+1)^{2p+1}\right)L_{kl}^{-(2p+1)}C_s=-1 \qquad \text{(B8)}$$

Setting the r series length M to N sets the p range from 1 to $N-1$, providing $N-1$ linear equations to solve for the $N-1$ C_s coefficients. Thus

$$\Psi\underline{C}_s=-\underline{u} \qquad \text{(B9)}$$

with

$$\psi_{ps}\equiv 2\left(2s^{2p+1}-(s-1)^{2p+1}-(s+1)^{2p+1}\right)L_{kl}^{-(2p+1)} \qquad \text{(B10)}$$

where Ψ is an $N-1$ by $N-1$ matrix whose pth row and sth column element is ψ_{ps}, $\underline{C}_s$ is an $N-1$ length column matrix whose elements

are the $N-1$ C_s coefficients, and $\underline{u}$ is an $N-1$ length column matrix with each element equal to 1. (Note: in [6] and other applications, $N = L_{kl}$. However, N can be larger than this as in [8]). Solving Eq. B9 for $\underline{C}_s$ finally yields

$$\underline{C}_s = -\Psi^{-1}\underline{u} \tag{B11}$$

References

[1] Jordan, J. W., "An Accurate Strapdown Direction Cosine Algorithm," NASA TN-D-5384, September 1969.

[2] Bortz, J. E., "A New Concept In Strapdown Inertial Navigation," Ph.D. Thesis, Massachusetts Inst. of Technology, Cambridge, MA, June, 1969.

[3] Goodman, L. E., and Robinson, A. R., "Effects of Finite Rotations on Gyroscope Sensing Devices," *Journal of Applied Mechanics*, Vol. 25, June 1958, pp. 210–213.

[4] Bortz, J. E., "A New Mathematical Formulation for Strapdown Inertial Navigation," *IEEE Aerospace and Electronic Systems Magazine*, Vol AES-7, No. 1, Jan. 1971, pp. 61–66.

[5] Laning, J. H., Jr., "The Vector Analysis of Finite Rotations and Angles," Massachusetts Inst. of Technology, Instrumentation Lab. Special Rept. 6398-S-3, 1949.

[6] Miller, R., "A New Strapdown Attitude Algorithm," *Journal of Guidance, Control, and Dynamics*, Vol. 6, No. 4, July–Aug. 1983, pp. 287–291. doi:10.2514/3.19831

[7] Ignagni, M. B., "Optimal Strapdown Attitude Integration Algorithms," *Journal of Guidance, Control, and Dynamics*, Vol. 13, No. 2, March–April 1990, pp. 363–369. doi:10.2514/3.20558

[8] Ignagni, M. B., "Efficient Class Of Optimized Coning Compensation Algorithms," *Journal of Guidance, Control, and Dynamics*, Vol. 19, No. 2, March–April 1996, pp. 424–429. doi:10.2514/3.21635

[9] Savage, P. G., *Strapdown Analytics-Second Edition*, Strapdown Associates, Inc., Maple Plain, Minnesota, 2007.

[10] Savage, P. G., "Strapdown Inertial Navigation System Integration Algorithm Design Part 1-Attitude Algorithms," *Journal of Guidance, Control, and Dynamics*, Vol. 21, No. 1, Jan.–Feb. 1998, pp. 19–28. doi:10.2514/2.4228

[11] Savage, P. G., "Strapdown System Algorithms," *Advances In Strapdown Inertial Systems*, NATO AGARD Lecture Series No. 133, May 1984, Section 3.

[12] Savage, P. G., "A New Second-Order Solution for Strapped-Down Attitude Computation," *AIAA/JACC Guidance and Control Conference*, AIAA, New York, Aug. 1966.

[13] Roscoe, K. M., "Equivalency Between Strapdown Inertial Navigation Coning and Sculling Integrals/Algorithms," *Journal of Guidance, Control, and Dynamics*, Vol. 24, No. 2, March–April 2001, pp. 201–205. doi:10.2514/2.4718